

**Highly efficient PMS activation by nZVI@MoS₂ via Mo-Fe interfaces
synergistic interaction for rapid degradation of ofloxacin**

Wanling Wu, Tingting Wang, Zitong Song, Xuena Chen, Yuang Liu, Donglin Zhao*

*Anhui Province Engineering Laboratory of Advanced Building Materials, School of
Materials and Chemical Engineering, Anhui Jianzhu University, Anhui, Hefei, 230026,
PR China*

*Corresponding author. Tel: 86-551-63828100, Fax: 86-551-63828103.

Email address: zhaodlin@126.com (Donglin Zhao)

Text S1 Materials

Ferric sulfate heptahydrate ($\text{FeSO}_4 \cdot 7\text{H}_2\text{O}$), Molybdenum (MoS_2 , 99.5%), Ofloxacin (OFL, 98%), PMS ($2\text{KHSO}_5 \cdot \text{KHSO}_4 \cdot \text{K}_2\text{SO}_4$), sodium thiosulfate ($\text{Na}_2\text{S}_2\text{O}_3 \cdot 5\text{H}_2\text{O}$), Sulfadiazine (SDZ), 2,4-dichlorophenol (2,4-DCP), Ciprofloxacin (CIP), methanol (MeOH), tert-butanol (TBA), p-Benzoquinone (p-BQ), L-Histidine (L-His), formic acid (HCOOH , HPLC \geq 99%), potassium dihydrogen phosphate (KH_2PO_4), sodium sulfate (Na_2SO_4), sodium nitrate (NaNO_3), sodium bicarbonate (NaHCO_3), sodium chloride (NaCl) and humic acid (HA) were purchased from Shanghai Maclin Biochemical Technology Co., Ltd. Sodium borohydride (NaBH_4) was obtained from Damao Chemical Reagent Factory (Tianjin, China). 5,5-dimethyl-1-pyrroflax-oxide (DMPO), 2,2,6,6-tetramethylpiperidine (TEMP) were bought from Aladdin Reagent Co., Ltd. (China).

Text S2 Characterization and analytical methods

The microstructure and elemental distribution of the nZVI@ MoS_2 composite were examined by scanning and transmission electron microscopy (SEM, GeminiSEM 500, ZEISS, Germany; TEM, HT7700, Hitachi, Japan), together with high-resolution TEM (JEM-2100, JEOL, Japan). Crystalline phases and surface functional groups were identified using X-ray diffraction (XRD, MXPAPHF, Japan) and Fourier transform infrared spectroscopy (FTIR-1500, USA), while the specific surface area and pore structure were determined by the Brunauer–Emmett–Teller (BET) method (Autosorb-iQ, Quantachrome, USA). Surface elemental composition and chemical states before and after reaction were analyzed by X-ray photoelectron spectroscopy (XPS, ESCALAB QXi, Thermo Scientific, USA). Transformation products of ofloxacin (OFL) were identified by liquid chromatography–mass spectrometry (LC–MS, 1290 II–6460, Agilent, USA), and mineralization efficiency was assessed by total organic carbon (TOC) analysis (Multi N/C

3100, Jena, Germany).

Reactive oxygen species generated in the nZVI@MoS₂/PMS system were detected using electron paramagnetic resonance (EPR, A300 EMX PLUS, Bruker, Germany). The experimental parameters were set as follows: magnetic field center at 3500 G; microwave frequency of 9.8 GHz; microwave power of 2.0 mW; modulation frequency of 4.0 G; modulation amplitude of 4.0 G; sweep width of 200 G; receiver gain of 3.54×10^4 ; time constant of 41.0 ms; sweep time of 15 s; and 15 scans were accumulated. DMPO was used as the spin-trapping agent for detecting •OH, SO₄^{•-} in aqueous solution, as well as O₂^{•-} in methanol. TEMP was employed as the spin trap to detect ¹O₂ in aqueous solution (Chen et al., 2024; Qi et al., 2025; Su et al., 2025).

The concentration of OFL was quantified by ultra-performance liquid chromatography (UPLC, 1260 Infinity II Prime, Agilent, USA) equipped with a C18 column and UV detection at 294 nm. The mobile phase consisted of 0.1% (v/v) formic acid in water and methanol (7:3), with a flow rate of 1.0 mL min⁻¹ at 30 °C. Real water matrices, including domestic well water and three Chaohu Lake samples (Anhui Province, China) with different pollution levels, were used to evaluate practical applicability.

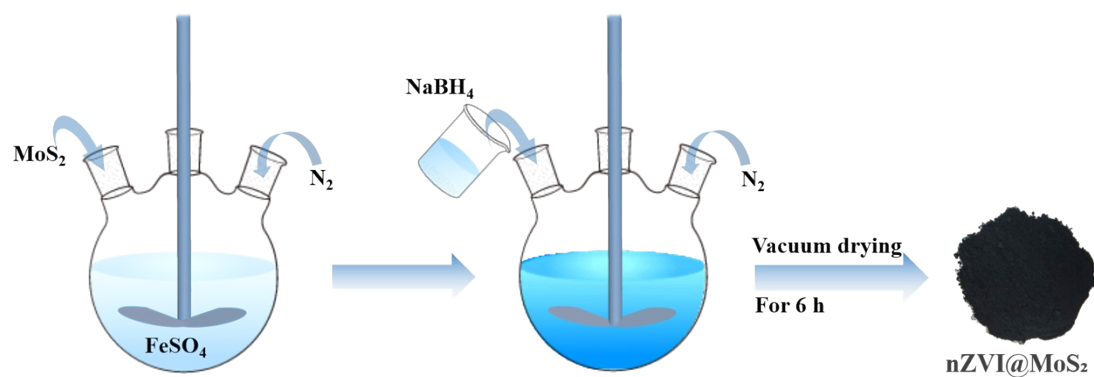


Fig. S1 Schematic for preparation of nZVI@MoS₂.

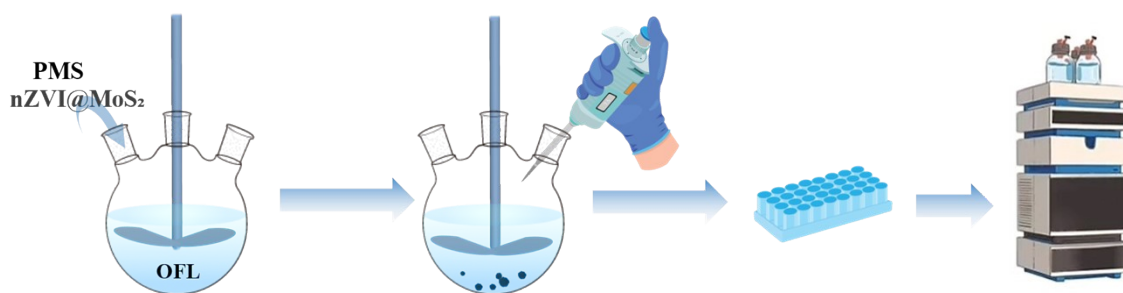


Fig. S2 Schematic diagram of the experimental process.

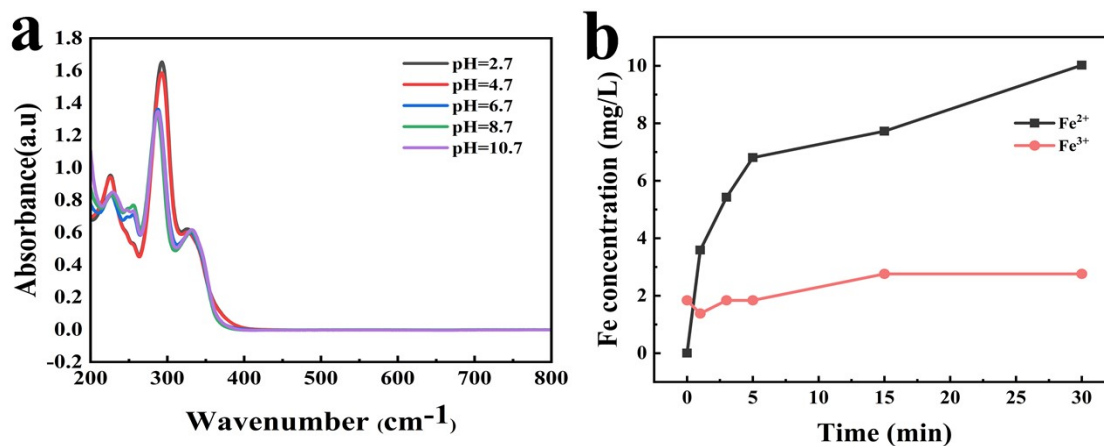


Fig. S3 (a) UV-Vis spectra of OFL under different pH conditions (2.7-10.7); (b) Concentrations of Fe^{3+} and Fe^{2+} in $\text{nZVI}@MoS_2/\text{PMS}$ system for degradation of OFL.

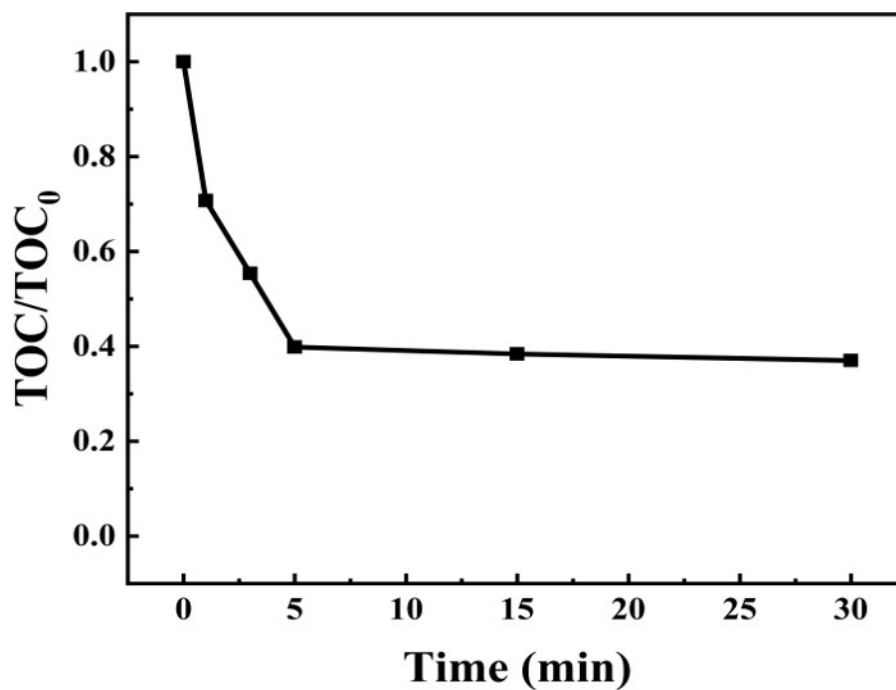
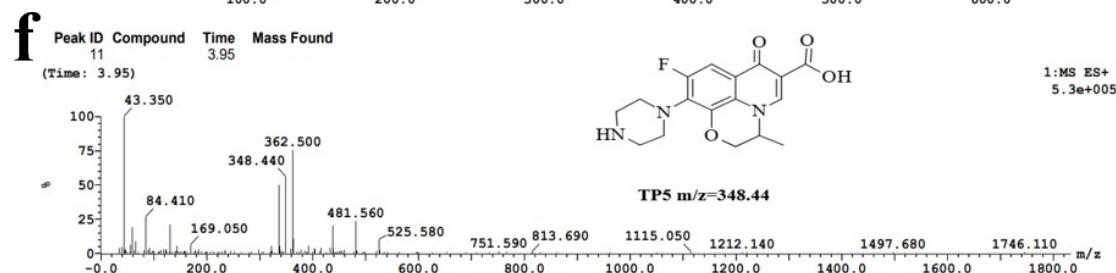
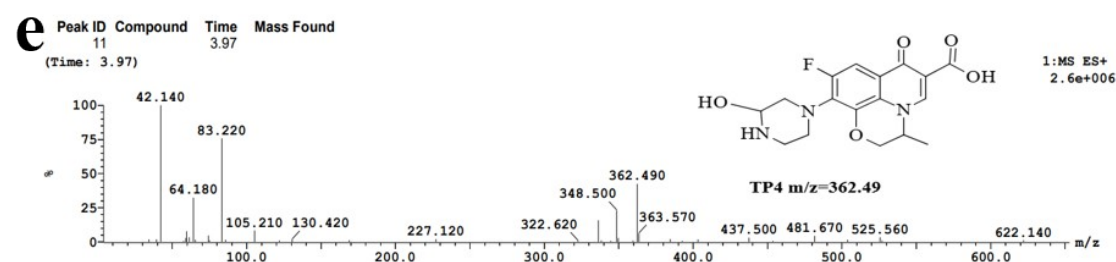
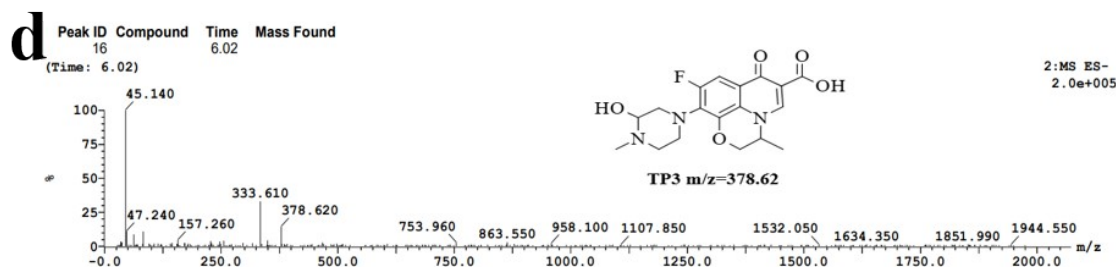
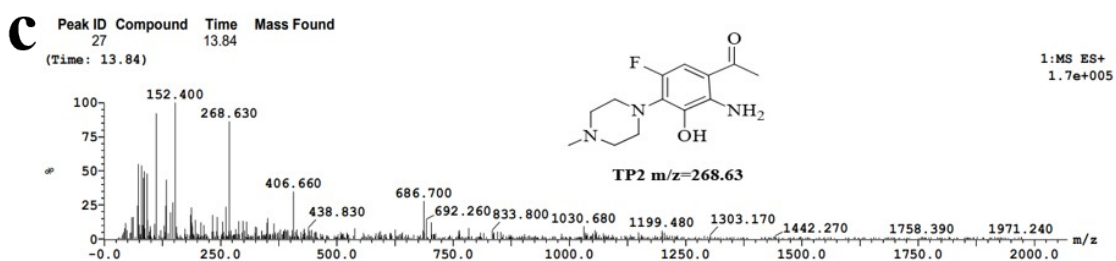
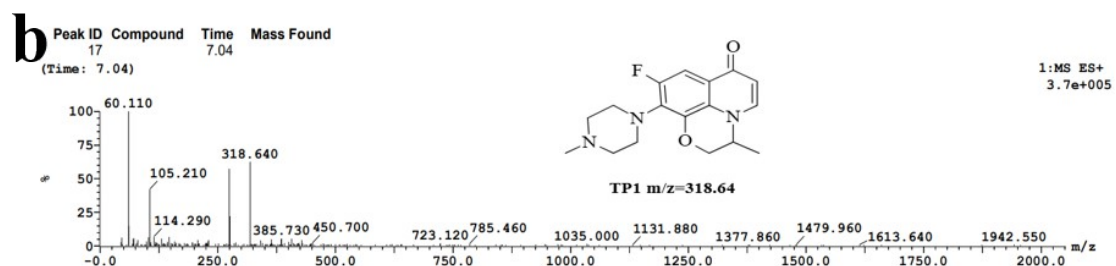
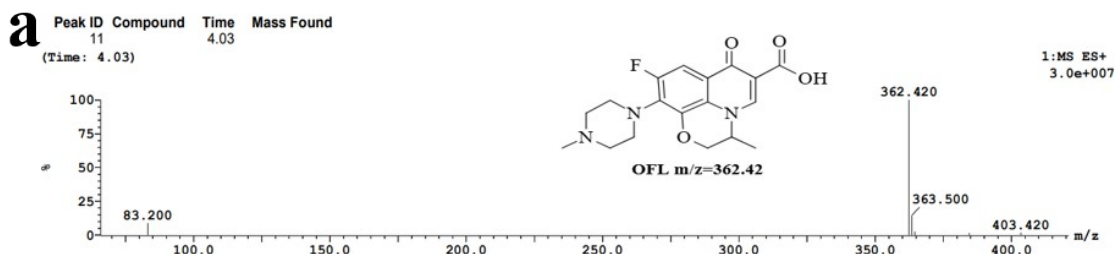


Fig. S4 Variation of TOC removal with reaction time for OFL in $\text{nZVI}@MoS_2/\text{PMS}$ system. Reaction conditions: $[\text{nZVI}@MoS_2] = 0.1 \text{ g/L}$, $[\text{PMS}] = 0.2 \text{ mM}$, Mo/Fe (20 wt% Mo), initial pH = 6.7, $[\text{OFL}] = 30 \text{ mg/L}$, $t = 25 \text{ }^\circ\text{C}$.



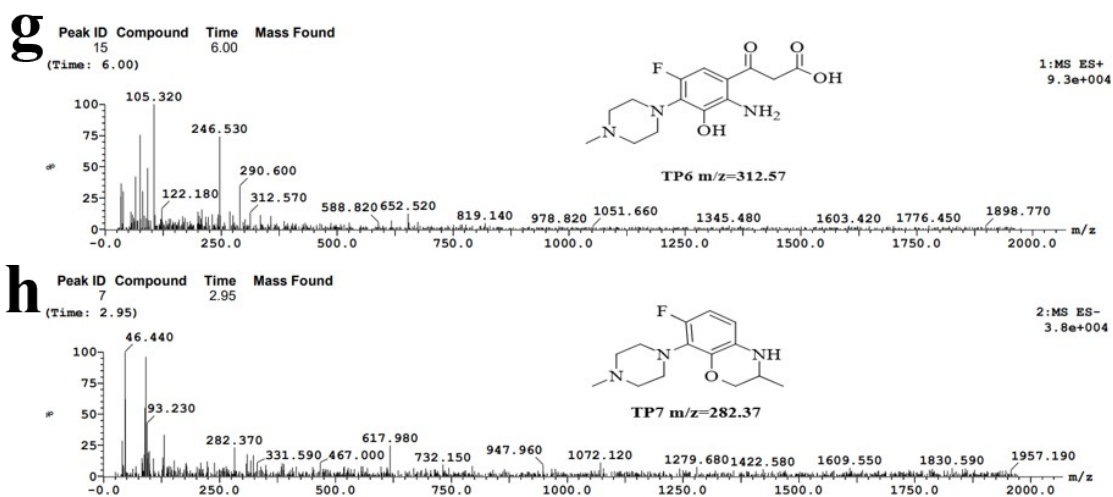


Fig. S5 LC-MS fragment patterns of OFL degradation intermediates by nZVI@MoS₂/PMS system.

Table S1

Surface area, pore size, and pore volume of the catalyst.

Catalyst	S _{BET} (m ² /g)	Pore size (nm)	Pore volume (cm ³ /g)
nZVI	14.72	1.54	0.06
MoS ₂	5.56	1.66	0.03
nZVI@MoS ₂	20.98	2.01	0.08

Table S2

Comparisons of OFL degradation in different systems.

Catalyst	Catalyst Dosage	PMS Concentration	OFL Concentration	Time (min)	Removal Efficiency (%)	References
LaFeO ₃ @ZIF-67	0.4 g/L	1 mM	20 mg/L	15	92.48%	(41)
CuFe ₂ O ₄ -Mt	0.4 g/L	2 mM	40 mg/L	60	85.2%	(40)
CoFe ₂ O ₄ /C	0.04 g/L	0.8 mM	20 mg/L	12	96.8%	(39)
nZVI@MoS ₂	0.1 g/L	0.2 mM	30 mg/L	30	97.4%	this study

Table S3

Index parameters of the lake water and domestic well water.

Water	Cl ⁻ (mg/L)	SO ₄ ²⁻ (mg/L)	NO ₃ ⁻ (mg/L)	PO ₄ ³⁻ (mg/L)
Lake water (Slight)	233.67	221.60	1.66	0.05
Lake water (Moderate)	249.54	265.46	1.54	0.04
Lake water (Severe)	277.25	253.16	3.98	0.21
Groundwater (Domestic well)	885.34	130.52	118.52	0.01

Table S4

ECOSAR toxicity analysis of OFL and intermediates.

Compound	Acute toxicity Logarithmic-transformed toxicity value			Chronic toxicity Logarithmic-transformed toxicity value		
	Fish (96hr LC50)	Daphnid (48hr LC50)	Green Algae (96hr EC50)	Fish	Daphnid	Green Algae
OFL	7.702	7.267	6.358	6.469	5.731	5.356
TP1	4.174	3.850	3.397	3.071	2.620	2.641
TP2	3.193	2.909	2.624	2.138	1.792	1.957
TP3	8.777	8.295	7.191	7.488	6.627	6.084
TP4	8.950	8.460	7.321	7.652	6.768	6.195
TP5	7.549	7.120	6.237	6.323	5.601	5.248
TP6	7.803	7.361	6.421	6.561	5.804	5.403
TP7	1.726	0.800	0.720	0.495	-0.286	0.240



References

- P. Chen, Z.L. Cheng, X.Z. Zhang, C.Q. Yan, J. Wei, F.C. Qiu, Y. Liu, Fe–Mn bimetallic catalyst to activate peroxymonosulfate (PMS) for efficient degradation of tetracycline: mechanism insights and application for pharmaceutical wastewater, *J. Cleaner Prod.* 445 (2024) 141365.
- X.Y. Qi, S.Y. Xu, L. Zhang, Q.Q. Cao, L.Q. Zhang, X.G. Shi, Y.W. Gu, C. Wang, NiFe₂O₄@MoS₂ heterojunction induces the changes of PMS activation mode in PMS/vis system for the directed generation of ¹O₂, *Sep. Purif. Technol.* 363 (2025) 132175.

X. Su, J. Han, Y.W. Huang, X.M. Wang, S.Y. Wang, Z.Y. Ge, H.C. Yuan, J.Y. Liu, X.R. Xiang, F. Xia, L. Lin, Y. Lan, J. Meng, Valorization of blueberry pomace and red mud to zero valent iron biochar for antibiotic degradation with diminishment of toxic reagents, *Bioresour. Technol.* 437 (2025) 133074.